Contribution from the Corporate Research Science Laboratory,
Exxon Research and Engineering Company, Linden, New Jersey 07036

Facile Syntheses of New Molybdenum and Tungsten Sulfido Complexes. Structure of $Mo_3S_9^{2-}$

WIE-HIN PAN, MICHAEL E. LEONOWICZ, and EDWARD I. STIEFEL*

Received March 26, 1982

Heating $(NH_4)_2MS_4$ (M = W, Mo) in *N*,*N*-dimethylformamide leads to the formation of the trinuclear ions $M_3S_9^{2-}$. Under similar conditions but in the presence of 1,2-ethanedithiol ($edtH_2$) or *o*-aminobenzenethiol ($abtH_2$) the dinuclear ions $M_2S_4(edt)_2^{2-}$ or $M_2S_4(abt)_2^{2-}$ are formed. The complex $(PPh_4)_2Mo_3S_9$ (Ph = C_6H_5) crystallizes in the space group $P1$ ($Z = 1$) with unit cell dimensions $a = 9.100$ (2) Å, $b = 10.531$ (5) Å, $c = 13.286$ (6) Å, $\alpha = 87.02$ (4)°, $\beta = 84.99$ (2)°, and $\gamma = 83.56$ (2)°. The structure shows two external tetrahedral MoS_4 units chelating a central square-pyramidal MoS unit. The Mo–Mo–Mo angle is 155.0 (1)°. Key distances (Å) are as follows: Mo–S(terminal to central Mo) = 2.086 (4); Mo–S(terminal to external Mo) = 2.134 (4), 2.145 (4), 2.136 (3), 2.148 (3); Mo–S(bridge to external Mo) = 2.231 (3), 2.247 (3), 2.251 (3), 2.234; Mo–S(bridge to central Mo) = 2.429(3), 2.369 (3), 2.389 (3), 2.388 (3); Mo–Mo = 2.982 (1), 2.924 (1). The cyclic voltammetry of the trinuclear complexes is reported. The complexes $M_3S_9^{2-}$ are formulated as mixed-valence VI, IV, VI compounds, and a mechanism is proposed for their formation.

The chemistry of Mo–S compounds has attracted much attention in the past,[1] and recent reports have revealed the new binary anions $Mo_3S(S_2)_6^{2-}$,[2] $Mo_2(S_2)_6^{2-}$,[2] $MoS(S_4)_2^{2-}$,[3] and $Mo_2S_4(S_2)(S_4)^{2-}$.[4] In these complexes Mo is bound to S in the form of sulfido (S^{2-}), persulfido (S_2^{2-}) or tetrasulfido (S_4^{2-}) ligands, illustrating the structural variety that is possible when the chemically versatile elements Mo and S are present.[5]

The simplest binary Mo–S moiety is the MoS_4^{2-} ion. While this ion has been known for many years, its chemical reactivity has only recently been appreciated. MoS_4^{2-} has found extensive use in the syntheses of heteronuclear Fe–Mo–S complexes such as $Fe(MoS_4)_2^{3-}$[6,7] and $Mo_2Fe_6S_9(SEt)_8^{3-}$.[8] In part the proliferation of compounds of these types is a result of attempts to find analogues of the Mo–Fe center of the nitrogenase enzyme system.[9] Indeed, some of the compounds prepared show spectroscopic (EXAFS and EPR) features[6,10] similar to those exhibited by the Fe–Mo center in the native enzyme[11] and in the isolated Fe–Mo cofactor.[12,13] However, interest in MoS_4^{2-} extends beyond its interaction with Fe as it also forms complexes with elements in the Ni, Cu, and Zn subgroups[14,15] as well as with Mo[16] itself. In many of these complexes, the MoS_4 moiety remains intact and can be regarded as a bidentate ligand.

In this paper we report the thermal reaction of MoS_4^{2-} in *N*,*N*-dimethylformamide, which yields the new binary Mo–S species $Mo_3S_9^{2-}$. The synthesis and properties of $Mo_3S_9^{2-}$ and its W analogue as well as the crystal structure of $(PPh_4)_2Mo_3S_9$ are presented. We also discuss the thermal reactions of MoS_4^{2-} and WS_4^{2-} with ethanedithiol ($edtH_2$) and *o*-aminobenzenethiol ($abtH_2$), which lead to $M_2S_4L_2^{2-}$ complexes (M = Mo, W) of which the W analogues are heretofore unreported.

Experimental Section

All solvents and reagents were used as obtained unless otherwise stated. Analyses were done by Galbraith Inc., Knoxville, TN, and by the Analytical and Information Division of Exxon Research and Engineering Co.,

$(NH_4)_2MoS_4$. $(NH_4)_2MoS_4$ was prepared by a procedure similar to that previously reported.[27] H_2S (SGP) was passed through an ammonium hydroxide solution (200 mL of concentrated NH_4OH/60 mL of H_2O) of $(NH_4)_6Mo_7O_{24}$ (Alfa, 20 g). The temperature rose to 55–60 °C, and H_2S bubbling was stopped as soon as the reaction mixture cooled to below ca. 50 °C. Crystalline $(NH_4)_2MoS_4$ was deposited by the time room temperature was attained. The container was stoppered and stored in the refrigerator overnight. The product was filtered, washed successively with small amounts of cold water, methanol, and ether, and air-dried; yield 25 g (85%).

$(NH_4)_2WS_4$. $(NH_4)_2WS_4$ was prepared with use of a slight modification of the procedure reported by Corleis et al.[28] Tungstic acid (Alfa, H_2WO_4; 21.5 g) was suspended in an NH_4OH solution (150 mL of concentrated NH_4OH/60 mL of H_2O), and H_2S was passed through while the solution was heated to 60 °C. After 30 min the suspension was filtered, the filtrate was reheated to 60 °C, and H_2S was passed through again. After about 2 h, 15 mL of concentrated NH_4OH was added and H_2S passed for a further 5 h. Some crystals of $(NH_4)_2WS_4$ formed, and the reaction mixture was stored in the refrigerator overnight. The yellow crystals were filtered, washed with ethanol and ether, and dried; yield ca. 12 g (40%).

$(PPh_4)_2Mo_3S_9$. Method A. $(NH_4)_2MoS_4$ (0.34 g, 1.3 mmol) and PPh_4Cl (0.52 g, 1.4 mmol) were dissolved in 10 mL of degassed DMF (Burdick and Jackson, distilled before use). Benzenethiol (Aldrich; 0.095 mL, 0.9 mmol) in 5 mL of degassed DMF was added to the above solution. The resulting solution was stirred and heated (ca. 90 °C) under argon. The reaction is usually complete after 1 h as determined by the disappearance of MoS_4^{2-} peaks (472 and 320 nm) in the electronic spectrum of the reaction solution. The dark red reaction mixture was filtered, and ether was added to the filtrate to incipient precipitation. A fine black crystalline product precipitated. This was filtered, washed with ether, methanol, and ether again, and air-dried. More ether was added to the filtrate and the solution allowed to stand overnight. The large black crystals that formed were filtered, washed with methanol and ether, and air-dried; total yield 0.45 g, 77%. Anal. Calcd for $C_{48}H_{40}P_2Mo_3S_9$: C, 45.9; H, 3.2; P, 4.9. Found: C, 46.2; H, 3.3; P, 4.9. The tetraethylammonium salt can be prepared in a similar manner with $N(C_2H_5)_4Br$ in place of PPh_4Cl.

Method B. $(N(C_2H_5)_4)_2Mo_3S_9$ can also be prepared by exactly the same procedure as method A except without the use of benzenethiol; yield 43%. Anal. Calcd for $C_{16}H_{40}N_2Mo_3S_9$: C, 23.0; H, 4.8; N, 3.3. Found: C, 22.8; H, 4.7; N, 3.4. The preparation of the PPh_4^+ salt by this method led to an impure product.

---

(1) Stiefel, E. I. *Prog. Inorg. Chem.* **1977**, *22*, 1.
(2) Müller, A. Bhattacharyya, R. G.; Eltzner, W.; Mohan, N.; Sarkar, S. *Chem. Uses Molybdenum, Proc. Int. Conf.* **1979**, *3*, 59.
(3) Simhon, E. D.; Baenziger, N. C.; Kanatzidis, M.; Dragnajac, M.; Coucouvanis, D. *J. Am. Chem. Soc.* **1981**, *103*, 1218.
(4) Clegg, W.; Christou, G.; Garner, C. D.; Sheldrick, G. M. *Inorg. Chem.* **1981**, *20*, 1562.
(5) Müller, A.; Jaegerman, W. *Inorg. Chem.* **1979**, *18*, 2631.
(6) McDonald, J. W.; Friesen, G. D.; Newton, W. E. *Inorg. Chim. Acta* **1980**, *46*, L79.
(7) Coucouvanis, D. *Acc. Chem. Res.* **1981**, *14*, 201.
(8) (a) Wolff, T. E.; Berg, J. M.; Hodgson, K. O.; Frankel, R. B.; Holm, R. H. *J. Am. Chem. Soc.* **1979**, *101*, 4140. (b) Christou, G.; Garner, C. D. *J. Chem. Soc., Dalton Trans.* **1980**, 2354.
(9) (a) Wolff, T. E.; Berg, J. M.; Holm, R. H. *Inorg. Chem.* **1981**, *20*, 174. (b) Armstrong, W. H.; Holm, R. H. *J. Am. Chem. Soc.* **1981**, *103*, 6246.
(10) Wolff, T. E.; Berg, J. M.; Warrick, C.; Hodgson, K. O.; Holm, R. H.; Frankel, R. B. *J. Am. Chem. Soc.* **1978**, *100*, 4630.
(11) Cramer, S. P.; Hodgson, K. O.; Gillum, W. O.; Mortenson, L. E. *J. Am. Chem. Soc.* **1978**, *100*, 3398.
(12) Cramer, S. P.; Gillum, W. O.; Hodgson, K. O.; Mortenson, L. E.; Stiefel, E. I.; Chisnell, J.; Brill, W. J.; Shah, V. K. *J. Am. Chem. Soc.* **1978**, *100*, 3814.
(13) Rawlings, J.; Shah, V. K.; Chisnell, J. R.; Brill, W. J.; Zimmermann, R.; Münck, E.; Orme-Johnson, W. H. *J. Biol. Chem.* **1978**, *253*, 1001.
(14) Müller, A.; Ahlborn, E.; Heinsen, H.-H. *Z. Anorg. Allg. Chem.* **1971**, *386*, 102.
(15) Callahan, K. P.; Piliero, P. A. *Inorg. Chem.* **1980**, *19*, 2619.
(16) Dilworth, J. R.; Zubieta, J. A. *J. Chem. Soc., Chem. Commun.* **1981**, 132.

0020-1669/83/1322-0672$01.50/0

$[N(C_2H_5)_4]_2W_3S_9$. With use of $(NH_4)_2WS_4$ both method A and method B for the preparation of the Mo analogue can be applied except that higher temperatures (110–130 °C) and longer reaction times (2–3 h) are employed. Both methods give golden yellow microcrystalline products in high yields (50–80%). A product by method B gave the following analysis. Calcd for $C_{16}H_{40}N_2W_3S_9$: C, 17.5; H, 3.6; N, 2.6. Found: C, 17.6; H, 3.5; N, 2.6.

$[N(C_2H_5)_4]_2W_3OS_8$. This compound was obtained as a byproduct during a synthesis of $W_3S_9^{2-}$. It apparently formed as a result of air leaking into the reaction flask. This compound was obtained as fine red orange microcrystals. Anal. Calcd for $C_{16}H_{40}N_2W_3S_8O$: C, 17.7; H, 3.7; N, 2.6. Found: C, 17.8; H, 3.7; N, 2.6.

Reactions of $(NH_4)_2MoS_4$ with Mercaptans (Other than Benzenethiol). The reactions were carried out by method A above. The stoichiometry used was one $(NH_4)_2MoS_4$ to three –SH groups.

Use of $HS(CH_2)_2O(CH_2)_2SH$, $HS(CH_2)_2S(CH_2)_2SH$, *t*-BuSH, and *p*-thiocresol led to the formation of $Mo_3S_9^{2-}$ (identified by its IR and electronic spectra) as a product with yields upward of 50%. When 1,2-ethanedithiol (edtH$_2$) or *o*-aminobenzenethiol (abtH$_2$) was used, the known[17] dimeric complexes $Mo_2S_4(edt)_2^{2-}$ and $Mo_2S_4(abt)_2^{2-}$ were respectively obtained. Anal. Calcd for $C_{20}H_{40}N_2Mo_2S_8$ $[(N(C_2H_5)_4)_2Mo_2S_4(edt)_2]$: C, 31.4; H, 6.3; N, 3.7. Found: C, 31.1; H, 6.6; N, 4.1. Calcd for $C_{28}H_{50}N_4Mo_2S_6$ $[(N(C_2H_5)_4)_2Mo_2S_4(abt)_2]$: C, 40.7; H, 6.1; N, 6.8. Found: C, 37.3; H, 5.6; N, 6.1. (Although the analysis for $(N(C_2H_5)_4)_2Mo_2S_4(abt)_2$ is unsatisfactory, its IR spectrum is nearly identical with that obtained from a previously prepared sample.[17])

Reactions of $(NH_4)_2WS_4$ with Mercaptans. The procedures were similar to those for the molybdenum analogues except a higher temperature (ca. 135 °C) was used. Only the reactions with edtH$_2$ and abtH$_2$ were studied. The products obtained were $W_2S_4(edt)_2^{2-}$ and $W_2S_4(abt)_2^{2-}$. Anal. Calcd for $C_{20}H_{48}N_2W_2S_8$ $[(N(C_2H_5)_4)_2W_2S_4(edt)_2]$: C, 25.5; H, 5.1; N, 3.0. Found: C, 25.7; H, 5.3; N, 3.1. Calcd for $C_{28}H_{50}N_4W_2S_6$ $[(N(C_2H_5)_4)_2W_2S_4(abt)_2]$: C, 33.5; H, 5.0; N, 5.6. Found: C, 34.1; H, 5.2; N, 5.6.

Physical Measurements. IR spectra were obtained as KBr pellets on a Perkin-Elmer 683 spectrometer and UV–visible spectra on a Perkin-Elmer 330 spectrometer. Spectra were obtained in acetonitrile (Burdick and Jackson, distilled over CaH$_2$) solutions.

Electrochemical Measurements. Cyclic voltammograms were obtained with a PAR Model 173 potentiostat to which was connected a PAR Model 175 universal programmer and a Hewlett-Packard Model 7094B X-Y recorder. A Beckman platinum-button electrode was used as the working electrode referenced to a saturated calomel electrode. A solution of 0.1 M $[N(n\text{-}Bu)_4]PF_6$ (Southwestern Analytical Chemicals) in DMF (Burdick and Jackson, distilled before use) was used as the electrolyte. A rough test for reversibility was made by comparison with the fully reversible ferrocene $\rightleftarrows$ ferrocenium redox couple. At a scan rate of 200 mV/s the peak-to-peak (E_a–E_c) separation of our ferrocene sample was 180 mV, indicating a significant *iR* drop between the reference and working electrodes. For the purpose of our preliminary study, we did not deem it necessary to correct for this and instead relied on the ferrocene standard as a reference for reversibility.

Structure Determination of $(PPh_4)_2Mo_3S_9$. 1. Data Collection. The compound crystallizes in the space group $P1$ (C_1^1, No. 1) with lattice constants $a = 9.100$ (2) Å, $b = 10.531$ (5) Å, $c = 13.286$ (6) Å, $\alpha = 87.02$ (4)°, $\beta = 84.99$ (2)°, $\gamma = 83.56$ (2)° with $V = 1259.3$ Å^3 and $Z = 1$ giving a calculated density of 1.66 g/cm^3. The experimental density was found to be 1.61 g/cm^3. Intensity data were obtained from a single crystal of approximate dimensions 0.4 × 0.4 × 0.1 mm with use of an Enraf-Nonius CAD4 diffractometer equipped with a graphite-monochromatized Mo Kα ($\lambda = 0.71073$ Å) radiation source. With use of ω scans (1.8° width), 5877 independent data ($0 < \theta \leq 28°$) were collected with 4353 independent observed intensities having $I \geq 2\sigma(I)$, where $I = S(C - RB)$ and $\sigma(I) = [S(C + R^2B) + (kI)^2]^{1/2}$, C is the total count recorded during the scan, $R = 2.0$ is the ratio of scanning time to the total background B, S is the scan rate, and $k = 0.05$ is a factor introduced to reflect instrument instability. From these data structure factors and their estimated standard deviations were computed with use of $|F_o| = (I/Lp)^{1/2}$ and $\sigma(|F_o|) = \sigma(I)/2|F_o|Lp$, where L and p are the Lorentz and polarization corrections.

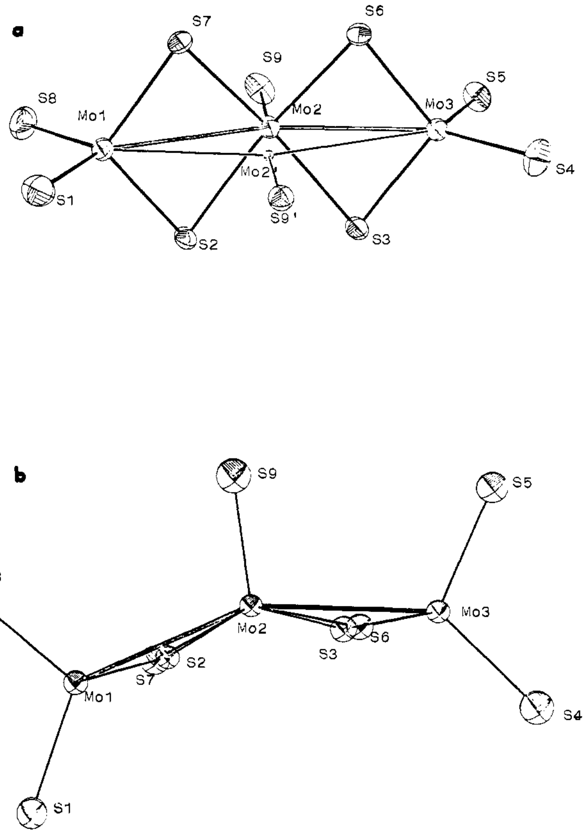

Figure 1. ORTEP drawings of $Mo_3S_9^{2-}$ (a) including and (b) excluding disorder positions. The disorder positions are indicated by the primed Mo and S atoms.

Intensities were not corrected for absorption (μ(Mo Kα) = 1.18 mm^{-1} with a calculated density of 1.66 g/cm^3), as ψ scans of several data displayed insignificant intensity fluctuations. Periodically monitored check reflections displayed no significant variation in intensity throughout the experiment.

2. Solution and Refinement of Structure. The structure was solved by the Patterson and Fourier techniques and refined (calculations were performed with use of the Enraf-Nonius Structure Determination Package, an integrated set of crystallographic computer programs for PDP 11 series computers) to a residual of ca. 7, where disorder of the central Mo2 and terminal S9 atoms (vide infra) became evident in the difference Fourier maps. Positions for the alternative atoms Mo2′ and S9′ were taken from the difference Fourier map and included along with Mo2 and S9 in the refinement at an occupancy of 0.10, as estimated from the electron densities in the map. The occupancy of Mo2 was then refined along with the other positional and thermal parameters until it converged to a value of 0.88. For the final cycles of least squares, the occupancies of Mo2 and S9 were set at 0.88 and the corresponding occupancies of Mo2′ and S9′ were held fixed at 0.12. Inclusion of calculated positions for the phenyl hydrogen atoms in the structure factor calculations led to a final conventional residual R_1 of 0.053 and a weighted residual $R_2 = (\sum w(|F_o| - |F_c|)^2/\sum w|F_o|^2)^{1/2} = 0.058$ with 565 parameters varied in the least squares and a data-to-parameter ratio of 7.7:1. The quantity minimized in the full-matrix least-squares analysis was $\sum w(|F_o| - |F_c|)^2$ with $w = \sigma(F)^{-2}$. Anisotropic temperature factors were applied to all non-hydrogen atoms except the 12% occupied atoms Mo2′ and S9′, which were refined isotropically. Hydrogen atom positional and isotropic thermal parameters were not refined. The final difference Fourier synthesis displayed maximum residual densities of 0.5 e/Å^3 at several places near the anion atoms. The final positional parameters of all non-hydrogen atoms are given in Table I. Thermal parameters for non-hydrogen atoms and hydrogen atom positions are available as supplementary material.

Results

Structure of $Mo_3S_9^{2-}$. Perspective views of the molecule are presented in Figure 1. The view in Figure 1a illustrates the geometry of the $Mo_3S_9^{2-}$ anion along with the nature of the

---

[17] Miller, K. F.; Bruce, A. E.; Corbin, J. L.; Wherland, S.; Stiefel, E. I. *J. Am. Chem. Soc.* **1980**, *102*, 5102.

Table I. Positional Parameters and Their Estimated Standard Deviations for $(PPh_4)_2Mo_3S_9$

atom	*x*	*y*	*z*
Mo1	0.3591 (1)	0.52678 (8)	0.71013 (7)
Mo2	0.5000 (0)	0.50000 (0)	0.50000 (0)
Mo3	0.7399 (1)	0.51273 (8)	0.33956 (7)
Mo2′	0.5896 (5)	0.5317 (4)	0.5561 (4)
S1	0.4363 (4)	0.5909 (3)	0.8438 (3)
S2	0.5127 (3)	0.3618 (2)	0.6519 (2)
S3	0.7194 (3)	0.3609 (2)	0.4641 (2)
S4	0.9600 (3)	0.5673 (4)	0.3213 (3)
S5	0.6748 (4)	0.4481 (3)	0.2011 (2)
S6	0.5806 (3)	0.6753 (2)	0.3964 (2)
S7	0.3749 (3)	0.6795 (2)	0.5864 (2)
S8	0.1367 (4)	0.4762 (4)	0.7369 (3)
S9	0.3396 (4)	0.4362 (3)	0.4177 (3)
S9′	0.754 (2)	0.607 (2)	0.637 (2)
P1	0.1190 (3)	0.0575 (2)	0.2485 (2)
P2	0.9725 (3)	0.9771 (2)	0.8062 (2)
C1	0.1659 (10)	0.0840 (9)	0.3737 (8)
C2	0.2775 (13)	0.0118 (10)	0.4160 (10)
C3	0.3224 (16)	0.0418 (13)	0.5111 (12)
C4	0.2453 (14)	0.1501 (11)	0.5583 (8)
C5	0.1308 (15)	0.2193 (12)	0.5140 (9)
C6	0.0954 (15)	0.1858 (13)	0.4230 (11)
C7	0.1480 (10)	0.1983 (8)	0.1707 (7)
C8	0.0584 (12)	0.2388 (8)	0.0921 (8)
C9	0.0920 (15)	0.3400 (11)	0.0286 (9)
C10	0.2229 (16)	0.3976 (11)	0.0393 (11)
C11	0.3054 (14)	0.3612 (10)	0.1173 (11)
C12	0.2715 (11)	0.2597 (9)	0.1832 (9)
C13	0.2361 (10)	−0.0741 (8)	0.1964 (8)
C14	0.2421 (12)	−0.1960 (9)	0.2469 (9)
C15	0.3341 (12)	−0.2954 (9)	0.2038 (10)
C16	0.4129 (12)	−0.2802 (9)	0.1139 (9)
C17	0.4050 (12)	−0.1631 (11)	0.0630 (8)
C18	0.3164 (10)	−0.0588 (9)	0.1053 (8)
C19	−0.0696 (8)	0.0278 (8)	0.2465 (7)
C20	−0.1113 (12)	−0.0847 (9)	0.2143 (8)
C21	−0.2524 (11)	−0.1045 (10)	0.2104 (9)
C22	−0.3658 (12)	−0.0132 (12)	0.2422 (10)
C23	−0.3275 (10)	0.0985 (11)	0.2792 (10)
C24	−0.1800 (11)	0.1187 (9)	0.2791 (9)
C25	0.9202 (11)	0.9457 (10)	0.6828 (7)
C26	0.9794 (15)	0.8259 (12)	0.6447 (10)
C27	0.9368 (17)	0.7984 (13)	0.5516 (12)
C28	0.8507 (16)	0.8862 (13)	0.4949 (10)
C29	0.7814 (14)	0.9898 (13)	0.5420 (9)
C30	0.8205 (13)	1.0270 (11)	0.6299 (9)
C31	0.9453 (11)	0.8387 (9)	0.8877 (8)
C32	0.8207 (11)	0.7739 (10)	0.8814 (11)
C33	0.7957 (11)	0.6763 (10)	0.9497 (11)
C34	0.8928 (13)	0.6376 (10)	1.0169 (11)
C35	1.0136 (16)	0.6987 (10)	1.0217 (10)
C36	1.0447 (12)	0.7987 (10)	0.9555 (9)
C37	0.8565 (10)	1.1130 (9)	0.8548 (8)
C38	0.8529 (11)	1.2279 (9)	0.8056 (9)
C39	0.7648 (12)	1.3327 (10)	0.8462 (10)
C40	0.6820 (13)	1.3132 (11)	0.9371 (10)
C41	0.6850 (12)	1.2002 (11)	0.9881 (9)
C42	0.7695 (11)	1.0993 (10)	0.9443 (8)
C43	1.1642 (11)	1.0080 (8)	0.8050 (8)
C44	1.1996 (10)	1.1188 (9)	0.8415 (8)
C45	1.3507 (12)	1.1364 (10)	0.8391 (10)
C46	1.4555 (11)	1.0489 (11)	0.8027 (8)
C47	1.4182 (13)	0.9355 (11)	0.7684 (11)
C48	1.2733 (11)	0.9153 (9)	0.7686 (9)

disorder in the structure involving the central Mo2 and terminal S9 atoms. Lines between Mo atoms do not necessarily imply that metal–metal bonding is present. The unprimed atoms represent the orientation of the molecule in 88% of the volume of the crystal, while Mo2′ and S9′ are the positions found in the remaining 12%. Bonds between the alternate atom Mo2′ and atoms S2, S3, S6, and S7 are omitted for clarity. The distances to the bridging sulfur atoms from Mo2′ and the geometry about this alternate atom site are equivalent to those of the more highly occupied Mo2 site. The somewhat higher dispersion among the distances and angles associated with Mo2′ and S9′ probably reflects an insensitivity of the least-squares refinement to the positions of the 12% occupied atom sites due to the reduction in scattering power of these atoms relative to that of the other atoms in the anion. This disorder problem has been encountered in the isostructural $W_3S_9^{2-}$ and $W_3OS_8^{2-}$[18,24] clusters.

Table II. Anion Bond Lengths (Å)[a]

Mo1–Mo2	2.982 (1)	Mo1–Mo2′	2.802 (5)
Mo3–Mo2	2.924 (1)	Mo3–Mo2′	3.082 (6)
Mo1–S1	2.134 (4)	Mo1–S7	2.247 (3)
Mo1–S2	2.231 (3)	Mo1–S8	2.145 (4)
Mo2–S2	2.429 (3)	Mo2′–S2	2.279 (6)
Mo2–S3	2.369 (3)	Mo2′–S3	2.372 (6)
Mo2–S6	2.389 (3)	Mo2′–S6	2.544 (6)
Mo2–S7	2.388 (3)	Mo2′–S7	2.376 (6)
Mo2–S9	2.086 (4)	Mo2′–S9′	2.15 (6)
Mo3–S3	2.251 (3)	Mo3–S5	2.148 (3)
Mo3–S4	2.136 (3)	Mo3–S6	2.234 (3)

[a] Estimated standard deviations in parentheses refer to the last significant digits.

The geometry around the central Mo can be described as a distorted square pyramid having a terminal sulfur at the apex and four sulfur atoms from two chelating MoS_4 units at its base. The angle Mo1–Mo2–Mo3 is 155.0°. The geometries of the sulfur ligands about the terminal Mo atoms are roughly tetrahedral. The bridging sulfur atoms, S2, S3, S6, and S7, together with the terminal Mo1 and Mo3 atoms approximately form a plane (rms deviation 0.04 Å). The central Mo2 atom is 0.62 Å above the S2, S3, S6, S7 plane.

Tables II and III report the bond distances and angles, respectively, of the anion. All metal–sulfur bond lengths are within expected bounds: terminal Mo–bridging S, 2.24 Å (average) central Mo–bridging S, 2.39 Å; central Mo–terminal S, 2.12 Å; terminal Mo2–terminal S, 2.14 Å. The Mo–Mo distances of 2.98 and 2.92 Å indicate a substantial assymetry in the structure, which is also reflected in some of the Mo–S distances. The cause of this asymmetry, which is also present[18a] in $W_3OS_8^{2-}$, is unknown. The nonbonded intramolecular contacts between bridging sulfur atoms lie within normal limits (S2–S7, 3.531 (4) Å; S2–S3, 2.991 (4) Å; S3–S6, 3.510 (4) Å; S6–S7, 3.007 (4) Å). The S–S contacts reveal that the central Mo has, in fact, a rectangular rather than a square-pyramidal structure. The Mo_2S_2 chelate rings are nonplanar with dihedral angles of 14.1° between the planes Mo1Mo2S2 and Mo1Mo2S7, 21.7° between the planes Mo2Mo3S3 and Mo2Mo3S6, 16.8° between planes S2Mo1S7 and S2Mo2S7, and 26.1° between planes S3Mo2S6 and S3Mo3S6.

Synthesis. The binary cluster complex $M_3S_9^{2-}$ is readily prepared by heating $(NH_4)_2MS_4$ (M = Mo, W) in the presence or absence of benzenethiol in DMF at 85 (Mo) or 130 °C (W) under anaerobic conditions. The Mo complex is black in crystalline form and brown in powdered form. The W complex, obtained as microcrystals, is golden yellow. The use of the ammonium salt of MS_4^{2-} as a starting material appears necessary. Attempts to prepare $Mo_3S_9^{2-}$ from $(AsPh_4)_2MoS_4$ in the presence or absence of benzenethiol failed.[18b] Neither

---

(18) (a) Secheresse, F.; Lavigne, G.; Jeannin, Y.; Lefebvre, J. *J. Coord. Chem.* **1981**, *11*, 11. (b) At the suggestion of a reviewer we have taken a DMF solution of $(NEt_3H)_2MoS_4$ and heated it at ca. 90 °C for ca. 1 h. The electronic spectrum of the reaction solution showed $Mo_3S_9^{2-}$ as the major product. This result is consistent with the proposed need for a proton in the reaction mechanism and shows that the NH_4 salt is not unique. We thank the reviewer for this suggestion.

(19) McKenna, S. T.; Pan, W.-H.; Miller, K. F.; Stiefel, E. I., unpublished results.

Table III. Anion Bond Angles (deg)[a]

S1-Mo1-S2	109.8 (1)	S2-Mo1-S7	104.1 (1)
S1-Mo1-S7	109.3 (1)	S2-Mo1-S8	110.8 (1)
S1-Mo1-S8	111.4 (2)	S7-Mo1-S8	111.1 (2)
S1-Mo1-Mo2	132.2 (1)	S1-Mo1-Mo2′	107.8 (2)
S2-Mo1-Mo2	53.2 (1)	S2-Mo1-Mo2′	52.4 (1)
S7-Mo1-Mo2	52.1 (1)	S7-Mo1-Mo2′	54.8 (1)
S8-Mo1-Mo2	116.4 (1)	S8-Mo1-Mo2′	140.7 (2)
S2-Mo2-S3	77.1 (1)	S2-Mo2′-S3	80.0 (2)
S2-Mo2-S6	150.8 (1)	S2-Mo2′-S6	150.3 (3)
S2-Mo2-S7	94.3 (1)	S2-Mo2′-S7	98.6 (2)
S3-Mo2-S6	95.1 (1)	S3-Mo2′-S6	91.1 (2)
S3-Mo2-S7	149.4 (2)	S3-Mo2′-S7	150.1 (4)
S6-Mo2-S7	78.1 (1)	S6-Mo2′-S7	75.3 (2)
S9-Mo2-S2	106.3 (1)	S9′-Mo2′-S2	106.5 (6)
S9-Mo2-S3	105.8 (2)	S9′-Mo2′-S3	105.5 (6)
S9-Mo2-S6	102.9 (1)	S9′-Mo2′-S6	103.2 (6)
S9-Mo2-S7	104.8 (2)	S9′-Mo2′-S7	103.5 (6)
Mo1-Mo2-Mo3	155.0 (1)	Mo1-Mo2′-Mo3	157.0 (3)
Mo1-Mo2-S9	105.5 (1)	Mo1-Mo2′-S9′	99.7 (6)
Mo3-Mo2-S9	99.5 (1)	Mo3-Mo2′-S9′	103.1 (6)
Mo1-Mo2-S2	47.3 (1)	Mo1-Mo2′-S2	50.8 (1)
Mo1-Mo2-S3	121.7 (1)	Mo1-Mo2′-S3	129.5 (2)
Mo1-Mo2-S6	123.4 (1)	Mo1-Mo2′-S6	124.8 (2)
Mo1-Mo2-S7	47.9 (1)	Mo1-Mo2′-S7	50.6 (1)
Mo3-Mo2-S2	124.9 (1)	Mo3-Mo2′-S2	124.1 (2)
Mo3-Mo2-S3	49.0 (1)	Mo3-Mo2′-S3	46.5 (1)
Mo3-Mo2-S6	48.5 (1)	Mo3-Mo2′-S6	45.6 (1)
Mo3-Mo2-S7	125.0 (1)	Mo3-Mo2′-S7	119.0 (2)
S3-Mo3-S4	110.8 (2)	S4-Mo3-S5	111.5 (2)
S3-Mo3-S5	110.4 (1)	S4-Mo3-S6	110.2 (1)
S3-Mo3-S6	103.0 (1)	S5-Mo3-S6	110.7 (1)
S3-Mo3-Mo2	52.5 (1)	S3-Mo3-Mo2′	49.9 (1)
S4-Mo3-Mo2	138.2 (1)	S4-Mo3-Mo2′	114.7 (2)
S5-Mo3-Mo2	110.4 (1)	S5-Mo3-Mo2′	133.8 (2)
S6-Mo3-Mo2	53.2 (1)	S6-Mo3-Mo2′	54.4 (1)
Mo1-S2-Mo2	79.5 (1)	Mo1-S2-Mo2′	76.8 (2)
Mo1-S7-Mo2	80.0 (1)	Mo1-S7-Mo2′	74.5 (2)
Mo2-S6-Mo3	78.4 (1)	Mo2′-S8-Mo3	80.1 (2)
Mo2-S3-Mo3	78.5 (1)	Mo2′-S3-Mo3	83.6 (2)

[a] Estimated standard deviations in parentheses refer to the last significant digits.

methanol nor acetonitrile were useful as solvents as no $Mo_3S_9^{2-}$ was formed possibly because even at reflux these solvents could not achieve the required temperature. Exclusion of both air and moisture is required especially in preparing the W complex. The presence of moisture and/or air leads to the formation of an orange complex formulated as $W_3OS_8^{2-}$. The elemental analysis and spectroscopic data indicate this compound to be the same as that recently reported[18a,20b] to have structure **1**, similar to that reported for $W_3S_9^{2-}$.[20a] **1** was

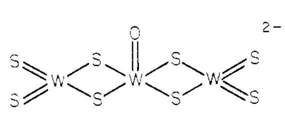

1

previously prepared[18a,20b] in aqueous solution, whence the crystalline PPh_4^+ complex was isolated[18a] as a 50:50 mixture of $W_3OS_8^{2-}$ and $W_3S_9^{2-}$. However, the $N(C_2H_5)_4^+$ salt of complex **1** could be obtained[18a] free of $W_3S_9^{2-}$ as indicated by its IR spectrum.

Table IV. Infrared and Electronic Spectroscopic Data

compd	IR,[a] cm^{-1}	UV-vis,[b] nm ($10^{-3}\epsilon$, $M^{-1}\ cm^{-1}$)
$(PPh_4)_2Mo_3S_9$	509 (m), 489 (m), 471 (w), 453 (sh, vw)	465 (18.0), 373 sh, 340 sh, 311 (26.4) sh
$[N(C_2H_5)_4]_2Mo_3S_9$	527 (m), 507 (s), 484 (s)	460 (13.5), 370 sh 338 sh, 307 (21.7) sh, 270 (29.3)
$[N(C_2H_5)_4]_2W_3S_9$	517 (m), 500 (sh), 492 (s), 479 (s), 465 (m), 434 (w)	392 (21.7), 325 sh, 285 sh, 271 (28.6), 241 (37.7)
$[N(C_2H_5)_4]_2W_3OS_8$	970 (s), 490 (s), 460 (m), 434 (w)	442 (9.8), 378 (28.0), 328 sh, 303 sh, 264 (32.5), 244 sh
$[N(C_2H_5)_4]_2$-$Pd(MoS_4)_2$[c]		467 (12), 380 sh, 348 (15), 312 (24), 274 sh, 268 (34)
$[N(C_2H_5)_4]_2$-$Pd(WS_4)_2$[c]		395 (21), 365 (21), 311 (21), 286 sh, 252 (20), 225

[a] KBr pellets. See text for tentative assignments. [b] CH_3CN solutions. [c] Reference 15.

The preparation of $[N(C_2H_5)_4]_2Mo_3S_9$ in the absence of benzenethiol leads to analytically pure product. However, the PPh_4^+ salt obtained by this method is impure as reflected by a high C, H analysis as well as by the IR spectrum, which indicates the possible presence of $(PPh_4)_2Mo_2S_4(S_2)_2$.[19] $(PPh_4)_2Mo_3S_9$ can be obtained in pure form when the reaction is carried out in the presence of benzenethiol.

For an assessment of the role, if any, of benzenethiol in the formation of $M_3S_9^{2-}$ from $(NH_4)_2MoS_4$, other thiols were used in place of benzenethiol. The use of the monothiols C_2H_5SH, t-C_4H_9SH, and *p*-thiocresol or the dithiols bis(mercaptoethyl) sulfide and bis(mercaptoethyl) ether led to $Mo_3S_9^{2-}$ in high yields. However, both edtH$_2$ and abtH$_2$ led to $Mo_2S_4^{2+}$- and $W_2S_4^{2+}$-containing species, also in relatively high yields. The first report[25] of the preparation of $[N(C_2H_5)_4]_2Mo_2S_4(edt)_2$ used $MoCl_3$ as the starting material and gave a yield of less than 7%. A subsequent report used $Mo_2(S_2)_6^{2-}$ as a starting material and gave a yield of over 80%.[17] The reaction of MoS_4^{2-} with edtH$_2$ also gives a high yield (ca. 70%) of $Mo_2S_4(edt)_2^{2-}$ and, in contrast to the case for the other preparations,[25,17] can be extended to the W analogue, leading to dinuclear complexes containing the $W_2S_4^{2+}$ core. The formation and properties of $M_2S_4^{2+}$ species from MS_4^{2-} will be discussed more extensively in forthcoming papers.

Spectroscopy. The compounds $M_3S_9^{2-}$ and $W_3OS_8^{2-}$ exhibit characteristic IR and UV-vis spectroscopic properties that serve to identify them. The spectra of the anions are tabulated in Table IV.

The anions $M_3S_9^{2-}$ show IR peaks below 600 cm^{-1} due to metal-sulfur vibrations. In $(PPh_4)_2Mo_3S_9$, the cation displays a very strong absorption at 525 cm^{-1}, which probably obscures a medium-intensity band arising from the anion. In the $N(C_2H_5)_4^+$ salt, where the cation shows no interfering absorption below 600 cm^{-1}, this band is observed at 527 cm^{-1}. The corresponding band in the W analogue appears at 517 cm^{-1}. This band is absent in $[N(C_2H_5)_4]_2W_3OS_8$, which instead shows a single very sharp and strong peak at 970 cm^{-1} arising from the W=O stretch (Table IV; see also ref 18). The peaks at 527 and 517 cm^{-1} for $Mo_3S_9^{2-}$ and $W_3S_9^{2-}$, respectively, are assigned to the M=S stretch of the central metal.

Other peaks in the IR spectra of $M_3S_9^{2-}$ (Table IV) are attributed to terminal M-S stretches in the MS_4 units and to M-S stretches within bridging M-S-M units. In $(PPh_4)_2Mo_3S_9$, the peaks at 509 and 489 cm^{-1} can be assigned

---

(20) (a) Koniger-Ahlborn, E.; Müller, A. *Angew. Chem., Int. Ed. Engl.* **1975**, *14*, 573. (b) Müller, A.; Rittner, W.; Neumann, A.; Koniger-Ahlborn, E.; Bhattacharya, R. G. *Z. Anorg. Allg. Chem.* **1980**, *461*, 91.

(21) Hanewald, K.; Gattow, G. *Z. Anorg. Allg. Chem.* **1981**, *476*, 159.

(22) Saxena, R. S.; Jain, M. E.; Mittal, M. L. *Aust. J. Chem.* **1968**, *21*, 91.

(23) Day, V. W.; Fredrich, M. F.; Klemperer, W. G.; Shum, W. *J. Am. Chem. Soc.* **1977**, *99*, 6146.

(24) Hanewald, K.; Kiel, G.; Gattow, G. *Z. Anorg. Allg. Chem.* **1981**, *478*, 215.

(25) Bunzey, G.; Enemark, J. H.; Howie, J. K.; Sawyer, D. T. *J. Am. Chem. Soc.* **1977**, *99*, 4168.

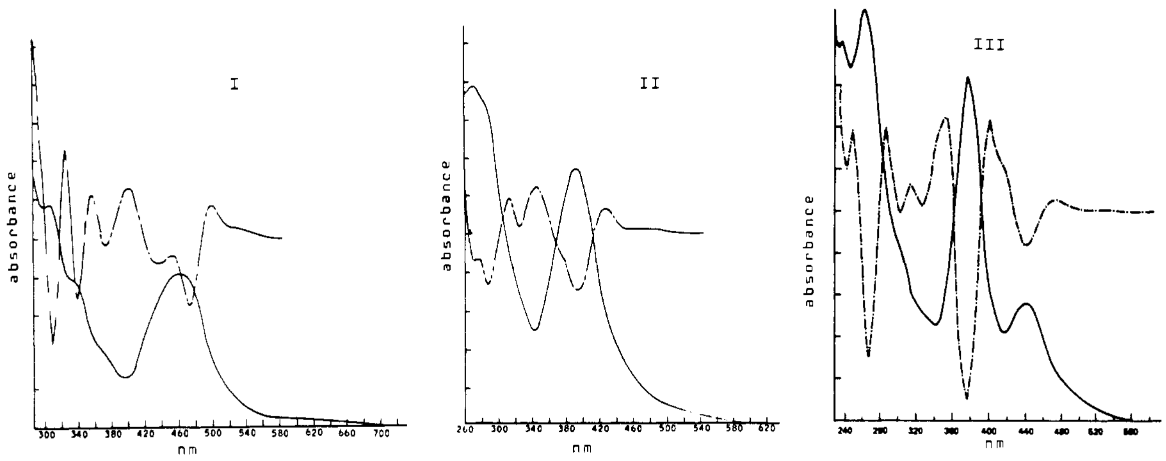

Figure 2. Electronic spectra of (I) $Mo_3S_9^{2-}$, (II) $W_3S_9^{2-}$, and (III) $W_3OS_8^{2-}$: (—) absorption; (---) second derivative of absorption.

Table V. Cyclic Voltammetric Data[a]

compd	$E°$(reversible),[b] V	irreversible waves	
		E_c(redn)	E_a(oxidn)
$(PPh_4)_2Mo_3S_9$	−1.15	−1.635, −1.95, −2.14	−0.32, −1.90
$[N(C_2H_5)_4]_2$-Mo_3S_9	−1.14	−1.54, −2.01	−0.34, −0.54, −1.87
$[N(C_2H_5)_4]_2$-W_3S_9	−1.42	−1.67, −2.38	−0.49, −0.71, −2.22
$[N(C_2H_5)_4]_2$-W_3OS_8	−1.68	−1.88	−0.71

[a] All potentials (E's) reported in volts. [b] $E° = (E_c + E_a)/2$: E_a = potential on anodic sweep; E_c = potential on cathodic sweep.

to symmetric and antisymmetric Mo═S stretches of the ligand MoS_4^{2-}. The increase in the terminal Mo═S vibrational energy from that of the free ligand MoS_4^{2-} (where ν(Mo═S) = 470 cm^{-1}) is generally observed when MS_4^{2-} species are ligated to a central metal atom as, for example, in $M'(MS_4)_2^{2-}$ species where M′ = Ni, Pd, Pt, and M = Mo, W.[15] The peaks at 471 and 453 cm^{-1} can be assigned to bridging Mo–S stretches although the former is somewhat higher than corresponding values in the square-planar $M'(MoS_4)_2^{2-}$ species (ca. 450 cm^{-1}). In $[N(C_2H_5)_4]_2Mo_3S_9$, the peak at 484 cm^{-1} is broad and, as a result, the peaks at 470 and 450 cm^{-1} are only observed as shoulders.

In $[N(C_2H_5)_4]_2W_3S_9$, the bands at 492 and 479 cm^{-1} are assigned to terminal W═S vibrations from the WS_4 moieties. The bridging W–S–W vibrations appear at 465 and 434 cm^{-1}. These assignments are comparable to those in the square-planar $M'(WS_4)_2^{2-}$ species. The splitting of the terminal W═S vibrational energies is apparently small in $W_3OS_8^{2-}$, and only a broad peak is observed at 490 cm^{-1}. However, the bridging W–S stretches are quite similar to those in $W_3S_9^{2-}$. Detailed assignments would be aided by isotopic labeling and complementary Raman scattering experiments.

The electronic spectra of the anions $Mo_3S_9^{2-}$, $W_3S_9^{2-}$, and $W_3O_8^{2-}$ are tabulated in Table IV and shown in Figure 2. In $Mo_3S_9^{2-}$, a very broad and unsymmetrical peak is observed near 460 nm. The second derivative of this peak allows its tentative resolution into two peaks at 472 and 435 nm. Other peaks appear as shoulders at lower wavelengths. In $W_3S_9^{2-}$, although the absorption at 392 nm appeared symmetrical, the second derivative shows it also to be composed of two almost overlapping peaks. Unlike the above, $W_3OS_8^{2-}$ shows two well-resolved peaks in the long-wavelength region. The peak near 442 nm serves a useful purpose. During the preparation of $W_3S_9^{2-}$, monitoring the electronic spectrum of the reaction solution allows the detection of $W_3OS_8^{2-}$ formed due to leakage of air into the reaction system.

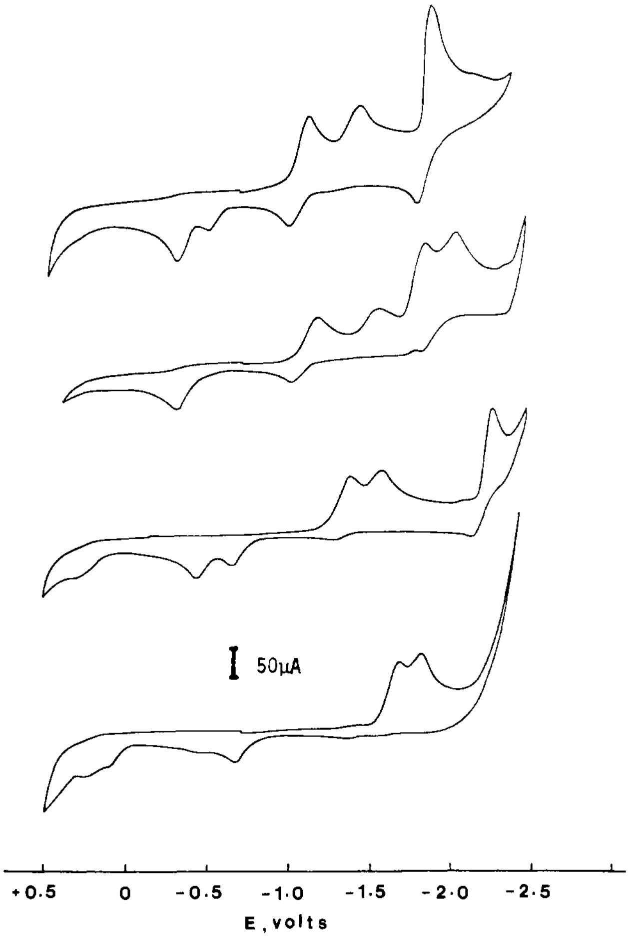

Figure 3. Cyclic voltammograms (respectively from top to bottom) of $[N(C_2H_5)_4]_2Mo_3S_9$, (1.8 mM), $(PPh_4)_2Mo_3S_9$ (2.6 mM), $[N(C_2H_5)_4]_2W_3S_9$ (1.8 mM), and $[N(C_2H_5)_4]_2W_3OS_8$ (2.1 mM) in DMF (containing 0.1 M $N(C_4H_9)_4PF_6$) vs. SCE. The scan rate was 200 mV/s between +0.5 and −2.5 V.

The electronic spectra of the species reported here are very similar to those reported for $M'(MS_4)_2^{2-}$ species,[15] and the absorption spectra for $Pd(MoS_4)_2^{2-}$ and $Pd(WS_4)_2^{2-}$ are included in Table IV for comparative purposes.

Cyclic Voltammetry. Cyclic voltammograms (CV) of the complexes $(PPh_4)_2Mo_3S_9$, $(NEt_4)_2Mo_3S_9$, $(NEt_4)_2W_3S_9$, and $(NEt_4)_2W_3OS_8$ were obtained in DMF solutions at concentrations of 1.8–2.6 mM. The results are summarized in Table V and Figure 3.

For the $M_3S_9^{2-}$ complexes, three reduction peaks are clearly observed. If the reduction scan is reversed before the second

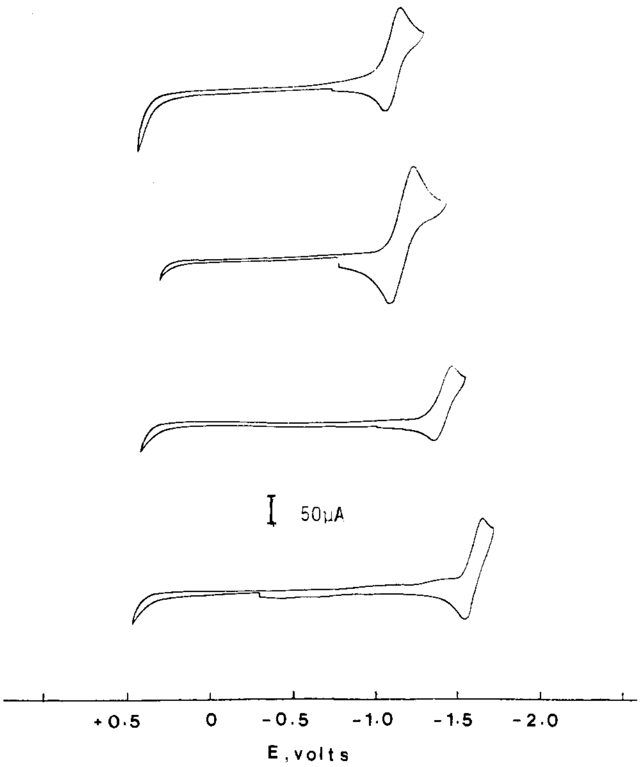

Figure 4. Cyclic voltammograms of the same compounds in the same respective order as in Figure 3 but with scans between +0.5, and −1.4 V, +0.4 and −1.5 V, +0.5 and −1.6 V, +0.5 and −1.8 V, respectively.

reduction occurs, the first reduction corresponds to a quasi-reversible one-electron reduction by the criterion of peak-to-peak separation (see Figure 4). Since the second reduction peak follows the first one closely, it interferes with a good measurement of the oxidation current of the first redox wave and an accurate measure of i_a/i_c is not possible. The two other reduction waves observed are irreversible. (The extra reduction peak in $(PPh_4)_2Mo_3S_9$, probably the one at −1.945 V, arises from the cation PPh_4^+. A CV of PPh_4Cl shows one irreversible reduction peak at −1.89 V).

In $(NEt_4)_2W_3OS_8$, only two reduction waves are observed down to −2.5 V. As in $M_3S_9^{2-}$, the first reduction wave appears as a reversible one-electron transfer (Figure 4) if the low-potential limit of the cycle is right after the first reduction wave. The reduction potentials of the first wave decrease in the order $W_3OS_8^{2-} > W_3S_9^{2-} > Mo_3S_9^{2-}$ (see Table V).

Discussion

Synthesis. The syntheses reported in this paper involve simple routes with mild conditions, leading to the formation of $Mo_3S_9^{2-}$ and $W_3S_9^{2-}$. While $Mo_3S_9^{2-}$ had previously not been reported, the preparation and characterization of $W_3S_9^{2-}$ had been described in a number of reports.[20,21] The previous[20,21] preparations of $W_3S_9^{2-}$ involved either the thermal decomposition of solid $(R_4X)_2WS_4$ (R = n-C_4H_{13}, n-C_6H_{13}, X = N; R = phenyl, X = P, As) or the heating of a mixture of $(NH_4)_2WS_4$ and PPh_4Cl or $AsPh_4Cl$.[20] Also, a dichloromethane solution of $[N(hexyl)_4]_2WS_4$ at room temperature was reported[21] to form $W_3S_9^{2-}$ in about 80 min in a reaction that is accelerated by the addition of an alkyl iodide. Accordingly, it was suggested[21] that alkylation of WS_4^{2-} bonds was a key feature of the mechanism of formation of $W_3S_9^{2-}$.

In the mode of preparation presented in this paper (at least in the case of the Mo complex), the reaction will not proceed if $(AsPh_4)_2MoS_4$ is used as the Mo starting material. The addition of $N(C_2H_5)_4Br$ in the beginning of our preparation is a convenience as the reaction proceeds just as well if $N(C_2H_5)_4Br$ is withheld until the reaction is completed. The presence of NH_4^+, which we presume to act as a proton donor, seems to be required.[18b]

Scheme I

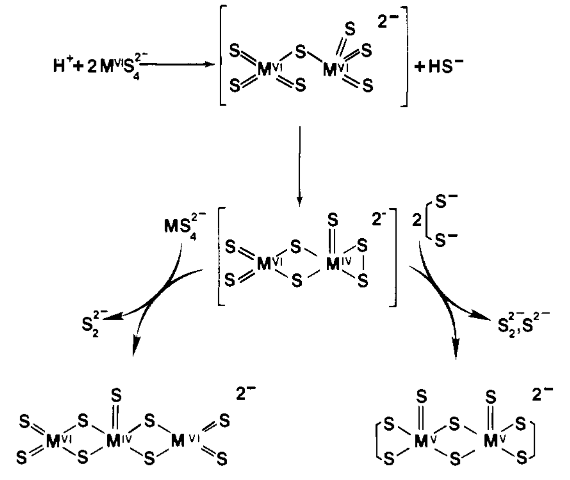

A tentative mechanism is outlined in Scheme I. The first step involves protonation (from NH_4^+) of MoS_4^{2-} to facilitate departure of SH^-, concomitant with dimerization to form an intermediate $Mo_2S_7^{2-}$ ion. The need for a proton at this stage may account for the lack of reactivity of $(AsPh_4)_2MoS_4$.[18b] The $Mo_2S_7^{2-}$ ion has previously been postulated[22] but has never been isolated. This ion may have a structure similar to that of the dimolybdate ion.[23] We postulate that $Mo_2S_7^{2-}$ is unstable toward isomerization to the intermediate, shown in Scheme I, via internal redox and ring closure. This intermediate may react by either of two pathways. First, if S_2^{2-} is displaced by MoS_4^{2-} acting as a bidentate ligand, the product is $Mo_3S_9^{2-}$. Alternatively, if $edtH_2$ or $abtH_2$ is present, both S_2^{2-} and S^{2-} (or their protonated analogues) can be replaced, leading to $M_2S_4^{2+}$-containing species.

Previous work[18a,20] shows that $W_3OS_8^{2-}$ forms in acidic aqueous solutions of WS_4^{2-}. It is probable, however, that $W_3S_9^{2-}$ is formed initially followed by a facile replacement of the central terminal sulfido ligand by an oxo ligand. In fact, it has been reported[21,24] that $W_3OS_8^{2-}$ could be prepared by simply recrystallizing $W_3S_9^{2-}$ in air. The formation of $W_3OS_8^{2-}$ from $W_3S_9^{2-}$ is probably slow since in the present study workup of the preparation of $W_3S_9^{2-}$ can be carried out in air and only a trace amount of oxo ligand (determined by the IR W=O stretch) is found in the product. However, $W_3OS_8^{2-}$ did form during an attempt to crystallize $W_3S_9^{2-}$ from a reaction solution that had been exposed to air for a few days. In contrast, exposing a solution of $Mo_3S_9^{2-}$ to air for a few days does not lead to $Mo_3OS_8^{2-}$. The substitution of the central S by O to form $Mo_3OS_8^{2-}$ may require heating in analogy to a similar subsitution in MoS_9^{2-}.[3]

Structure and Bonding of $Mo_3S_9^{2-}$. The terminal thiomolybdate ligands have tetrahedral coordination and are of dimensions similar to those of the MoS_4^{2-} ligands bound to first-row mono- and divalent transition-metal ions. The central Mo–S linkage is reminiscent of the central linkage in $MoS(S_4)_2^{2-}$ recently reported by Coucouvanis and co-workers.[3] The central Mo–S bond length of 2.086 Å can be compared to the 2.128-Å distance in MoS_9^{2-}.

The structural comparisons with $Ni(MoS_4)_2^{2-}$ and $MoS(S_4)_2^{2-}$ lead us to formulate the complex in terms of a central Mo(IV) ion flanked by two Mo(VI) ions (VI, IV, VI) rather than a V, VI, V assignment. The VI, IV, VI formulation leads to the electronic structural picture illustrated in Figure 5. The central Mo has a square-pyramidal structure with one short Mo–S linkage at the apical position. This linkage is likely to dominate the d-orbital splitting by analogy with the dominance of the electronic structure by the Mo=O linkage in oxo-

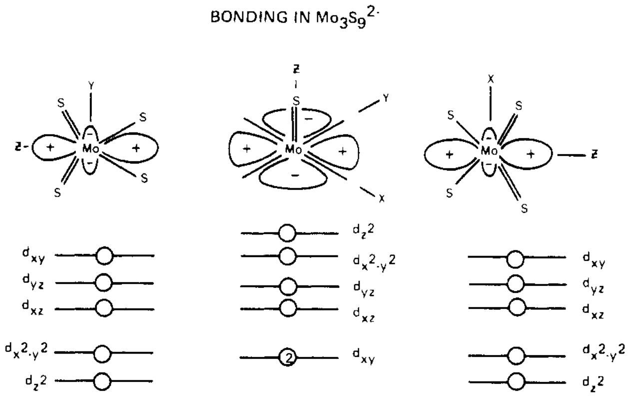

Figure 5. Molecular orbital picture of the Mo-Mo interactions in $Mo_3S_9^{2-}$.

molybdenyl complexes.[26] The splitting expected on the basis of coordinate system shown places the $4d_{xy}$ level lowest in energy, and the diamagnetism of the complex would require both d electrons of the central Mo(IV) to occupy that level. However, the $(4d_{xy})^2$ configuration may be significantly stabilized by the thiomolybdate ligands. Recent studies[7] indicate that MoS_4^{2-} may function as an acceptor ligand, moving electron density from the $(4d_{xy})^2$ configuration to empty MoS_4^{2-} levels. If the MoS_4^{2-} ion is oriented with its z axis bisecting S-Mo-S angles and roughly in the Mo-Mo direction, then, as shown in Figure 5, strong overlap is possible between the central Mo d_{xy} orbital and the d_{z^2} levels on the terminal Mo atoms. The $4d_{xy} \rightarrow 4d_{z^2}$ bonding is not of π character as there is no nodal plane containing the bond axis. However, the acceptor ability of MoS_4^{2-} may nonetheless be an effective stabilizing feature of the $Mo_3S_9^{2-}$ complex. That there may be interaction between the central Mo and terminal Mo is indicated by the short Mo-Mo distance and more so by the small folding along the bridging sulfurs, S3-S6 and S2-S7.

Conclusion

The trinuclear clusters $M_3S_9^{2-}$ can readily be prepared by heating $(NH_4)_2MS_4$ in DMF. The structure of $(PPh_4)_2Mo_3S_9$ shows ligating MoS_4 groups and a central thiomolybdenyl group. The complexes are formulated as $(M^{VI}S_4)_2M^{IV}S^{2-}$, i.e., a mixed-valence formulation. The Mo-Mo distances may be indicative of inter-molybdenum charge transfer mediated by the d orbitals of the Mo atoms. Spectroscopically, the $M_3S_9^{2-}$ complexes behave similarly to $M'(MS_4)_2^{2-}$ (M' = Ni, Pd, Pt) complexes. The dinuclear complexes $M_2S_4(edt)_2^{2-}$ and $M_2S_4(abt)_2^{2-}$ can be prepared by heating MS_4^{2-} and $edtH_2$ or $abtH_2$ in DMF. The formation of the di- and trinuclear complexes from MS_4^{2-} may involve a common mechanism in which initial formation of the intermediate species $M_2S_7^{2-}$ is followed by internal redox processes leading to disulfide formation. Future studies will address both electronic structural features of these complexes and mechanistic aspects of their reactions.

Supplementary Material Available: Listings of cation bond lengths and angles, least-squares planes, structure factor amplitudes, anisotropic thermal parameters for non-hydrogen atoms, and calculated positional parameters for H atoms (37 pages). Ordering information is given on any current masthead page.

---

(26) Gray, H. B.; Hare, C. R. *Inorg. Chem.* **1962**, *1*, 363.
(27) Kruss, G. *Justus Liebigs Ann. Chem.* **1884**, *225*, 29.
(28) Corleis, E. *Justus Liebigs Ann. Chem.* **1886**, *232*, 244.

Contribution from the Departments of Chemistry, Howard University, Washington, DC 20059,
American University, Washington, DC 20016, and University of Virginia, Charlottesville, Virginia 22901

Nitration of Metal Ion Coordinated Imidazole and the Crystal Structure of Pentaammine(4-nitroimidazolato)cobalt(III) Chloride

C. B. STORM,*[1a] C. M. FREEMAN,[1a] R. J. BUTCHER,*[1a] A. H. TURNER,[1a] N. S. ROWAN,[1b] F. O. JOHNSON,[1b]
and E. SINN[1c]

Received February 26, 1982

The title complex, $[Co(NH_3)_5(NO_2Im)]Cl_2$, was prepared by the action of a standard HNO_3-H_2SO_4 nitrating mixture on $Co(NH_3)_5(ImH)^{3+}$. The complex has been characterized by ^1H NMR and UV-vis spectroscopy and a single-crystal X-ray structure determination. The pH dependence of the ^1H NMR spectra has been determined, and the pK_a of the coordinated NO_2Im is 1.66. Crystal data for $[Co(NH_3)_5(NO_2Im)]Cl_2$ is as follows: space group $P2_1/n$; $Z = 4$; $a = 9.434$ (2), $b = 13.679$ (3), $c = 10.457$ (3) Å; $\beta = 93.65$ (2)°; $V = 1346.7$ (5) Å^3; $R = 4.5\%$ for 2135 reflections.

Introduction

The electrophilic aromatic nitration of nitrogen heterocycles is a useful route to nitro, amino, and fluoro derivatives for these compounds. These derivatives have many uses as drugs, synthetic intermediates, or analogues in structure-activity investigations. The amino acid histidine occurs in most proteins and is of considerable importance in protein structure and function. The imidazole functional group of histidine is widely used as an intrinsic probe of protein structure-activity relationships[3] and is quite suitable for chemical modification for both large and small perturbations on its chemical and spectroscopic properties.[4]

The coordination of a ligand to a metal ion can cause an appreciable change in reactivity of the ligand.[2] Metal ion coordinated imidazole has been shown to have a pK_a of 10.0 and to have a much reduced rate of C-2 H exchange and ^1H and ^{13}C NMR spectra quite different from free imidazole.[5,6] We wish to report here the regiospecific nitration, under very mild conditions, of imidazole coordinated to Co(III). The facile nitration and the pK_a of the resulting complex support

---

(1) (a) Howard University. (b) American University. (c) University of Virginia.
(2) Busch, D. H. "Reactions of Coordinated Ligands"; American Chemical Society: Washington, DC, 1963; Adv. Chem. Ser. No. 37.
(3) Markley, J. L. *Acc. Chem. Res.* **1975**, *8*, 70.
(4) Yeh, H. J. C.; Kirk, K. L.; Cohen, L. A.; Cohen, J. S. *J. Chem. Soc., Perkin Trans. 2* **1975**, 928.
(5) Harrowfield, J. M.; Norris, V.; Sargeson, A. M. *J. Am. Chem. Soc.* **1976**, *98*, 7282.
(6) Rowan, N. S.; Storm, C. B.; Rowan, R., III. *J. Inorg. Biochem.* **1981**, *14*, 59.

0020-1669/83/1322-0678$01.50/0